Global NEST Journal, Vol 25, No 1, pp 47-56

Investigation of copper ion adsorption using activated sawdust powder: Isotherm, kinetic and thermodynamic studies

Ilavarasan N.[1], Srinivasa Rao Y.S.[2], Gokulan R.[3*], and Aravindan A.[4]
[1]Department of Civil Engineering, University College of Engineering, Anna University, BIT Campus, Tiruchirappalli, Tamil Nadu, India
[2]Department of Mechanical Engineering, Sri Sivani College of Engineering, Srikakulam, Andhra Pradesh, India
[3]Department of Civil Engineering, GMR Institute of Technology, Rajam, Andhra Pradesh – 532 127, India
[4]Department of Civil Engineering, Koneru Lakshmaiah Educational Foundation, Guntur, Andhra Pradesh – 522 502, India
Received: 24/09/2022, Accepted: 23/10/2022, Available online: 31/10/2022
*to whom all correspondence should be addressed: e-mail: gokulravi4455@gmail.com
https://doi.org/10.30955/gnj.004496

Graphical abstract

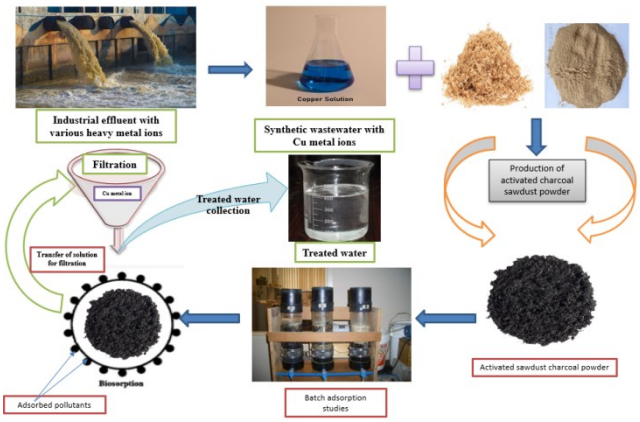

Abstract

The batch adsorption technique investigated the efficiency of sawdust adsorbent for removing copper ions from synthetic solutions. A chemical synthesis process prepared the activated sawdust powder, and its surface area and pore volume were obtained by BET isotherm analysis. The ability of copper ion uptake by activated sawdust powder was examined under the characterization study of SEM, EDX & FTIR studies. Various isotherm studies checked the process of adsorption, and the kinetic studies confirm the nature of the adsorption process with sawdust adsorbent. Thermodynamic studies were used to analyze the endothermic nature of the adsorption process, and 0.3 N of H_2SO_4 acid desorbs 93.27% of copper ions from the spent adsorbent. The experimental study confirms the better adsorption ability of sawdust powder in the activated charcoal form to remove the heavy metal pollution in aqueous solutions.

Key words: Biosorption, sawdust powder, copper ions, isotherm & kinetic studies.

1. Introduction

Water pollution is one of the emerging problems we are still facing from earlier days. Clean water is essential to all living creatures for their survival. Changes in water's physical and chemical characteristics create harmful effects on humans and animals. Due to the rapid growth of industrial activities and a huge amount of product production, the industries used clean water for manufacturing and cleaning purposes (Sasireka *et al.*, 2021). Many pollutants such as dyes, heavy metals, bacterial growth and other non-degradable elements have been presented in the industrial effluent, contaminating the natural water bodies while discharging from the industries. Among these pollutants, heavy metals play an important role in water pollution released from tanneries, electroplating and pulp & paper industries (Halim *et al.*, 2019). Heavy metal ions released from the industries, such as cadmium, copper, chromium, arsenic, lead, etc., accumulate in effluents. These are very harmful to the surroundings and create severe effects even in very low concentrations. Consumption of polluted water may create long-term effects on all living beings and increases the severity of the surrounding environment.

Developing an innovative treatment process at a very low cost has been a basic need in recent days, and many treatment technologies are available to treat the primary pollutants in the water. Chemical precipitation, Membrane filtration, Ion exchange, Adsorption, Coagulation and flocculation are the most common treatment methods available to remove the non-degradable toxic pollutants from wastewater. Among these methods, adsorption has been used widely recently, and no secondary sludge was developed during the treatment process (Batagarawa *et al.*, 2019). Selecting the adsorbate material is one of the important techniques to increase the efficiency of the adsorption rate. Many organic and inorganic materials were used, such as groundnut shells, orange & banana peels, Seeds of various plants, Fly ash and, industrial sewage sludge etc (Yahya *et al.*, 2020). In this research, sawdust powder activated carbon has been used to remove the copper (Cu^{2+}) metal ion concentrations from the synthetic solutions using the batch adsorption technique. The maximum allowable limit of copper metal ion is

1.3 mg/L for drinking water, 1 mg/L for sewage systems and 0.25 mg/L for water reuse. The sawdust adsorbent is an organic material available in local sawmills produced during the process of wood furniture and other related materials. It is a waste product for fire resistance material produced in large quantities while processing the woods and it has very high stability in temperature (Alam Khan *et al.*, 2022). Hence, it is decided to use this material to remove the copper ion concentration from the synthetic solution. The adsorption process was conducted through batch mode, and the performance of prepared adsorbent material has been evaluated in various characterization techniques. Table 1 represents the various heavy metal ions and their adsorption using a sawdust-based adsorbent material.

2. Materials and methods

Table 1. Research works conducted using sawdust-based adsorbents

S. No.	Type of pollutant (s)	Metal ion uptake	Ion concentration	Ideal pH	adsorbent dose	Time of contact	Reference
1.	Cu^{2+}	64.37%	20 mg/L	2.0	0.6 g/L	90 min	In this study
2.	Cr^{6+}	71.29%	4 mg/L	3.0	5 g/L	60 min	Sirusbakht *et al.*, 2018
3.	Fe^{2+} & Mn^{2+}	87%	300 mg/L	5.0	300 mg/10 mL	150 min	Jatinder *et al.*, 2018
4.	Zn^{2+}	90%	10 mg/L	5.0	0.5 gm	60 min	Pragati *et al.*, 2015
5.	Pb^{2+}	99.63%	100 ml	5.0	0.25 g	30 min	Khalid *et al.*, 2019
6.	Cu^{2+}	91.74 mg/g	30 mg/L	4.0	1 g/L	60 min	Eleryan *et al.*, 2022
7.	Cr^{3+}	65.83%	20 mg/L	5.0–7.0	1 g/L	60 min	Gunatilake *et al.*, 2016

2.1. Stock solution & adsorbent preparation

For stock solution preparation, 100 mg of copper sulphate ($CuSO_4$. $5H_2O$) powder was added with 1 lit of distilled water to make the concentration 100 mg/L. For batch studies, the concentration was adjusted based on the experimental needs. For adsorbent preparation, the sawdust was collected in the local sawmills and washed several times to eliminate the dust and other particles. The sample was dried in sunlight for up to 10 hours and placed in the muffle furnace for 24 hours at a temperature of 200°C. The charcoal adsorbent was taken from the oven and washed with double distilled water to eliminate the pollutants and other materials. Then, the adsorbent material was placed in an oven for further heating at 80°C and taken for batch experimental studies.

2.2. Characterization of activated sawdust powder

The surface area of activated sawdust powder was evaluated using the process of nitrogen adsorption at -196°C temperature. The activated adsorbent was allowed to heat at 300°C for 5 hours to remove the gas molecules, and Brunauer calculated the vacuum and the area of the surface–Emmett–Teller (BET) analysis. The relationship of Dubinin–Radushkevich (D–R) process the micro and meso pores and their sizes were obtained using the equation 1.

$$S_m = S_{BET} - S_u \quad (1)$$

Here, S_m and S_u represent the adsorbent's average micro and meso pore sizes and the S_{BET} average surface area obtained from BET analysis. Under the relative pressure of $P/P_o \sim 0.99$, the pore volume (VT) and amount of liquid nitrogen were obtained, and the volume of micro and meso pores was calculated using equation 2.

$$V_m = V_T - V_u \quad (2)$$

The pore distribution of the prepared adsorbent was evaluated by Barrett–Joyner–Halenda (BJH) model using the mean pore diameter D_P. Equation 3 can be used to find out the mean diameter of sawdust powder.

$$D_P = \frac{4\ V_T}{S_{BET}} \quad (3)$$

FTIR analyses were performed with 20 mg/L initial Cu^{2+} ion concentration, pH of 6.0 and 1 gm of activated sawdust powder to check the presence of various functional groups in the prepared adsorbent. The solution was placed in the shaker and shaken for 3 hours at 200 rpm speed to attain the proper mixing without forming any flocs. Then the sample was allowed into a complete settlement, and the final suspension was taken into the other experimental process. The FTIR range was fixed at the interval of 4 cm^{-1}, and the analysis was performed within 400 – 4000 cm^{-1} band level with 20 scans. Scanning Electron Microscopic (SEM) analysis was conducted to confirm the presence of pollutants on the adsorbent's surface, and the Energy Dispersive X-ray analysis was used to check the presence of targeted pollutant adsorption on the activated sawdust charcoal surface.

2.3. Batch isotherm studies

The efficiency of adsorption using activated sawdust charcoal powder has been evaluated by varying the parameters such as pH, adsorbent dose, contact time, initial concentration of metal ion solutions and temperature. Keeping the other parameters at a constant level and adjusting the pH from 2.0 to 7.0, the impact of changes in adsorption efficiency was evaluated to determine the optimum pH level. Similarly, the impact of adsorption efficiency was evaluated by changing the metal ion concentrations from 20 – 100 mg/L and keeping the other parameters at a constant level with optimum pH. To find the optimum level of adsorbent dose, the concentration of activated sawdust powder was adjusted from 0.5 to 2.5 g/L, and the contact time between adsorbent and adsorbate was varied from 10 to 120 minutes. The suspension was allowed into continuous stirring for up to 1 hour to reach the equilibrium condition.

The number of copper ions adsorbed by the adsorbent was calculated using equation 4 at the equilibrium time.

$$q_t = \frac{(C_o - C_t)\,V}{m}\ mg/g \quad (4)$$

Here, the number of copper metal ions adsorbed by the sawdust adsorbent was denoted by q_t, C_t denoted the concentration of adsorption study, the volume of copper ion solution was denoted by V, and the mass of the system was represented by m. The metal ion-containing solution was placed in a shaker another 5 minutes after the equilibrium time of 1 hour and allowed for identifying the concentration level using AAS (AA6300). Each analysis was done up to 2 times to get the concurrent value, and the mass balance of the adsorption system can be evaluated by using equation 5.

$$\%\ \text{Removal} = \left[\frac{C_o - C_e}{C_o}\right] X100 \quad (5)$$

Here, the C_o and C_e represent the initial and final concentrations of copper ion-containing solution at the equilibrium time.

2.4. Isotherm studies

During the equilibrium conditions, the isotherm studies evaluated the transmission of adsorbate from the solution to the adsorbent phase with the help of mathematical equations. Isotherm studies identified the adsorption sites & molecules and their interaction (Langeroodi *et al.*, 2018). The following types of isotherm studies were used in this work to determine the behavior of sawdust charcoal powder with the targeted metal ion uptake.

2.4.1. Langmuir isotherm

The gas & adsorbent phases and their equilibrium were explained by the Langmuir isotherm study based on the fluid and solid concentrations. Also, the process of adsorption changes has been described in this study. According to Langmuir's isotherm study, the adsorption process follows monolayer type on the activated adsorbent surface at the time of relative pressure and heterogeneous nature (Benjelloun *et al.*, 2021). The basic assumption of this model is the binding mechanism of copper ions, and sawdust adsorbent happens through chemical reactions. The linear equation of this isotherm study can be expressed in equation 6.

$$\frac{C_e}{q_e} = \frac{1}{K.q_{max}} + \frac{C_e}{q_{max}} \quad (6)$$

C_e denoted the concentration of the solution, the number of copper ions adsorbed per gram was denoted by q_e, and the constants of this model related to capacity and intensity were represented by K & q_{max}.

2.4.2. Freundlich isotherm

At a given temperature of 30°C, the adsorption variations in the adsorbed gas amount by unit mass of activated charcoal adsorbent were examined through the system pressure. This isotherm study has allowed multiple-layer adsorption based on the heterogeneous nature of the metal ion uptake process (Amit Kumar *et al.*, 2022). The linear equation of the Freundlich isotherm model can be expressed in equation 7.

$$\ln q_e = \ln k_f + \frac{1}{n}\ln C_e \quad (7)$$

The quantity of adsorbate adsorbed per gram was denoted by q_e, the Energy of adsorption was denoted by n, K_f denoted the Adsorption capacity, and Ce represented the solution's equilibrium concentration.

2.4.3. Sips isotherm

The combined process of the Langmuir and Freundlich isotherm model is called the sips model and can be used for heterogeneous site prediction within the limiting behavior (Yaseen *et al.*, 2018). This study completely ignored the adsorbate concentration and followed the monolayer adsorption process. The linear equation of this isotherm study can be expressed in equation 8.

$$\frac{1}{q_e} = \frac{1}{Q_{max}K_s}\left(\frac{1}{C_e}\right)^{\frac{1}{n}} + \frac{1}{Q_{max}} \quad (8)$$

The capacity of adsorption and constant of equilibrium was denoted by Q_{max} & K_s, and the heterogeneity factor was represented by n.

2.5. Kinetic studies

The detailed description of the solute release rate from the aqueous medium to the solid interface based on the given optimum adsorption parameters has been investigated through adsorption kinetic studies (Fideles *et al.*, 2019). This study obtained the process of adsorption due to weak or strong forces. The following common kinetic studies have been used in all kinds of adsorption to check the process, either physical or chemical mode.

2.5.1. Pseudo first order study

Within the solid and liquid systems, a solid adsorption capacity was developed. This has been evaluated by the pseudo-first-order or Lagergren model based on the assumption that the driving force is directly proportional to the metal ion desorption (Venkatraman *et al.*, 2021). The copper ion uptake by sawdust charcoal powder has been evaluated using the differences in initial and equilibrium concentrations (q_e & qt). The pseudo-first-order kinetic model can be expressed in equation 9.

$$\frac{dq_e}{dq_t} = k(q_e - q_t) \quad (9)$$

Applying the boundary conditions in equation 9, the metal ions adsorbed by sawdust charcoal powder were evaluated by calculating qe & qt.

The equation 9 can be rearranged to equation 10 after applying the boundary conditions.

$$\log(q_e - q) = \log q_e - \frac{k}{2.303}t \quad (10)$$

2.5.2. Pseudo second order study

The availability of active sites in the activated sawdust charcoal adsorbent is directly proportional to the amount of copper ions adsorption. Based on this assumption, the pseudo-second-order study was used to evaluate the performance of the adsorption process. The equation for the Pseudo 2nd order kinetic model can be expressed in equation 11.

$$\frac{d_q}{d_t} = k(q_e - q)^2 \quad (11)$$

The boundary conditions of t = 0 to t > 0, and q = 0 to q > 0 has been applied in the equation 11 and this can be rearranged to equation 12.

$$\frac{t}{q} = \frac{1}{h} + \frac{1}{q_e}t \quad (12)$$

The initial adsorption rate was denoted by $h = kq_e^2$; the rate constant was denoted by k. The constants of q_e, k and h were evaluated by using the linear plots of this model.

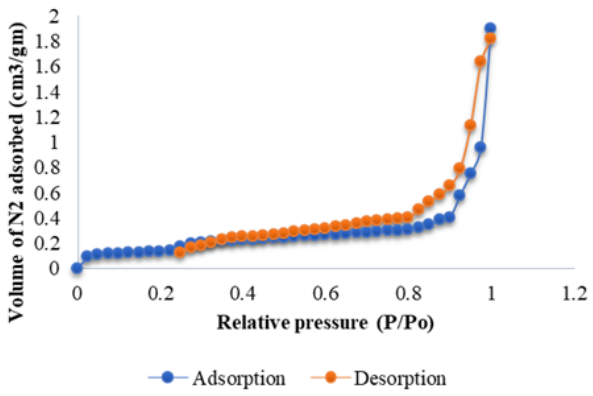

Figure 1. BET adsorption isotherm study of activated sawdust powder

3. Results and discussion

3.1. Surface area and pore distribution

Figure 1 shows the isotherm curve of adsorption and desorption rate of nitrogen at -196°C to evaluate the size of pores and surface area of activated sawdust charcoal adsorbent. Referring to Figure 1, it was confirmed that the process of adsorption followed the type – II category, indicating the presence of micro and meso pores (Saruchia *et al.*, 2019). The first curve indicates the produced adsorbent has micropores, and the second curve indicates the presence of meso pores in the sawdust adsorbent. The size of meso and micropores of sawdust adsorbent powder is listed in Table 2, and the surface area of activated sawdust powder is 4.25 m^2/g, which is lower than the other commercial activated carbons.

3.2. FTIR

The presence of functional groups has been evaluated using FTIR studies to check the ability to adsorb metal pollutants from aqueous solutions. Figure 2 (a) & (b) shows the FTIR image of raw and activated sawdust charcoal powder with various functional groups. The very high bandwidth energy from 3420 cm^{-1} to 2860 cm^{-1} produced in the analysis may confirm the presence of -OH and $-CH_2$ functional elements. The bandwidth from 1800 – 1000 cm^{-1}, various elements such as water at 1620 cm^{-1}, vibrations due to aromatic compounds at 1600 – 1400 cm^{-1}, bending vibrations due to $-CH_2$ element at 1400 – 1380 cm^{-1} and vibrations due to C-O stretching at 1080 cm^{-1} were identified. Also, the aromatic ring vibrations were observed at 1000 cm^{-1} level due to -C-H bending, and in lower frequency levels, the -OH stretching may be developed. The bandwidth and stretching vibrations of the adsorbent confirm the presence of various functional groups and its ability to adsorb the pollutants from aqueous solutions (Ambaye *et al.*, 2021).

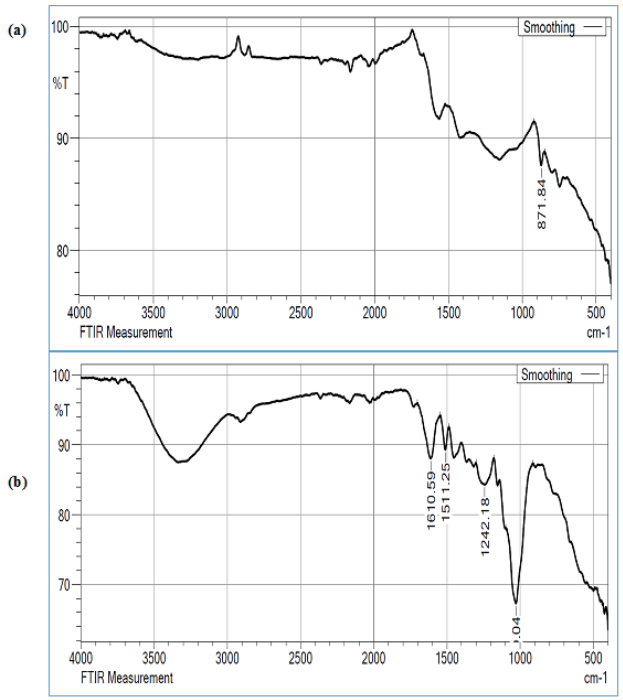

Figure 2. FTIR spectrum of (a) Raw adsorbent & (b) Activated charcoal adsorbent

Table 2. Pore characteristics of raw and activated sawdust powder

S.No	Description	Activated Sawdust biochar
1.	BJH surface area (m2/g)	81.273
2.	Pore volume (cc/g)	0.121
3.	Pore Radius (Å)	33.572
4.	BET surface area (m2/g)	4.25
5.	Average pore diameter (nm)	0.061

3.3. SEM analysis

The scanning electron microscope image of activated charcoal adsorbent before and after metal ion uptake was shown in Figure 3 (a) & (b), respectively. Before passing the metal ion-containing solution into the adsorbent, many active sites were available on the adsorbent's surface (Figure 3a). These active sites play an important role in receiving the pollutants from the aqueous medium. The copper ion-containing solution was allowed into the sawdust adsorbent and allowed for the adsorption process

up to the saturation time. Figure 3b shows the SEM image of activated saw dust adsorbent's surface after the copper ion uptake. Many active sites were filled with pollutants on the surface of the adsorbent, and there were no vacant sites available after the saturation point (Priya *et al.*, 2022). The pollutants were settled at the top of the adsorbent surface and formed a cloud shape showing the process of adsorption.

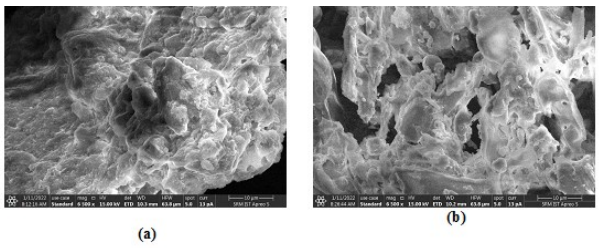

Figure 3. SEM image of activated sawdust charcoal powder (a) Before Cu^{2+} adsorption & (b) After Cu^{2+} adsorption

3.4. EDX analysis

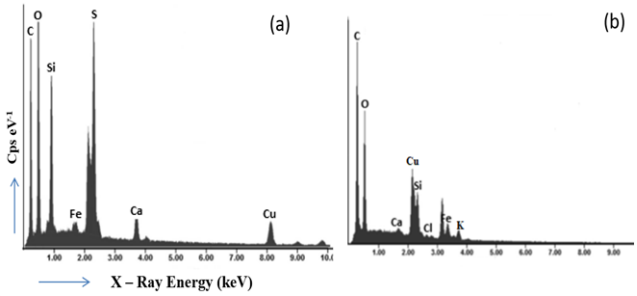

Figure 4. EDX images of activated sawdust charcoal powder (a) Before Cu^{2+} adsorption & (b) After Cu^{2+} adsorption

The adsorption of copper metal ions on the surface of the adsorbent was evaluated by EDX analysis. Figure 4 (a) & (b) shows the EDX images of sawdust adsorbent before and after copper metal ion uptake from the aqueous solutions. The EDX image of sawdust adsorbent before copper ion uptake shows various organic and inorganic elements such as carbon, oxygen, calcium etc. Figure 4b shows the EDX image of sawdust adsorbent after passing the metal ion solutions, and the presence of targeted metal ion (Cu^{2+}) was observed by referring to the image. Furthermore, the other organic and inorganic elements, such as Ca, Si, Fe etc., was observed from the EDX analysis.

3.5. Impact of adsorption by varying pH

The initial concentration of copper metal ion-containing solution was taken in 20 mg/L with 1 g/L activated sawdust powder dose, contact time of 60 minutes, and temperature of 30°C. The effect of metal ion adsorption efficiency was investigated by varying the pH from 2.0 to 7.0. The changes in adsorption efficiency by varying the pH of metal ion-containing solution was shown in Figure 5. When the pH of the metal ion solution is very low, the maximum amount of copper metal ions was observed an increase in pH can reduce the metal ion adsorption from the synthetic solution. During the low pH, the positively charged ions can react with negatively charged particles which may increase the rate of adsorption (Feszterová *et al.*, 2021). The hydroxide precipitation is very high in the higher pH values, which reduces the amount of copper metal ion uptake from aqueous solutions. Around 63.25% of copper metal ions were observed at an optimum pH level of 2.0 in this batch study.

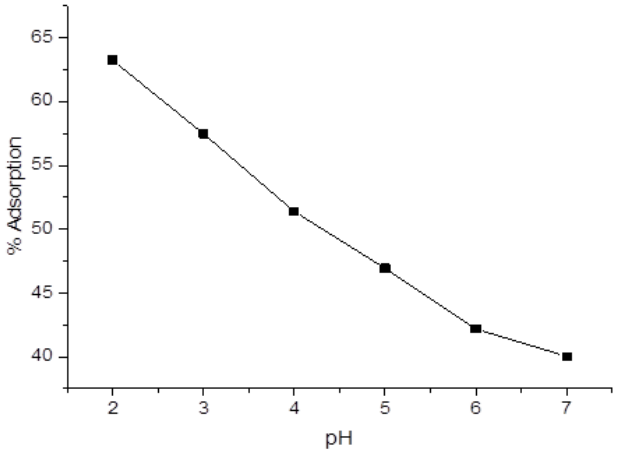

Figure 5. Impact of chromium metal ion uptake by varying the pH

3.6. Impact of adsorption by varying adsorbent dose

Taking the optimum pH of 2.0 and fixing the concentration of copper ion solution at 20 mg/L with a contact time of 60 minutes and temperature of 30°C, the activated sawdust charcoal powder dose was adjusted from 0.1 to 1 g/L for this study. The effect of copper ion uptake by varying the adsorbent dose is shown in Figure 6. During the initial stages, the metal ion uptake by the adsorbent was rapid, and a sudden decrement was noticed after 0.6 g/L of adsorbent dose. At higher concentrations of adsorbent dose, the availability of active sites is high, increasing the amount of pollutant uptake in aqueous solutions (Pholosi *et al.*, 2019). After the saturation point, the active sites are filled with pollutants, and there are no vacant sites on the adsorbent's surface. About 65.05% of copper metal ions were removed at an optimum dose of 0.6 g/L, and beyond that, the concentration gradient was developed at higher dose levels, reducing the copper ion uptake.

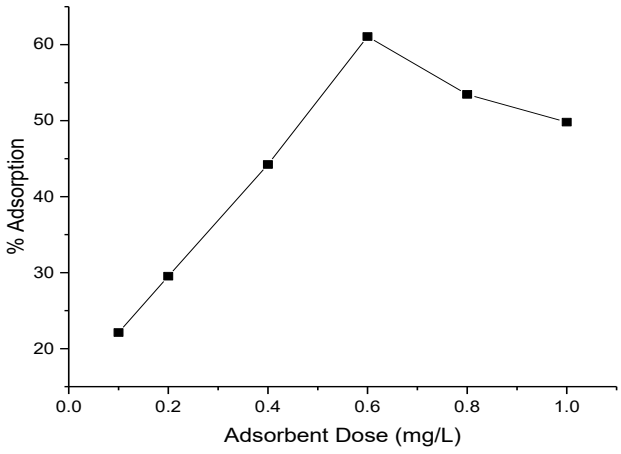

Figure 6. Impact of chromium metal ion uptake by varying the adsorbent dose

3.7. Impact of adsorption by varying the ion concentration

The copper metal ion concentrations in synthetic solution were adjusted from 20 to 100 mg/L, and the contact time was fixed at 60 minutes under 30°C temperature the impact of copper ion uptake by sawdust adsorbent has been investigated with optimum pH of 2.0 and adsorbent dose of 0.6 g/L. Figure 7 shows the impact of copper adsorption by varying the concentrations of metal ions in aqueous solutions. The maximum amount of adsorption was achieved by decreasing the concentrations of metal ion solutions because of the very low availability of active sites in sawdust powder. The adsorption efficiency gradually decreased with an increase in initial metal ion concentrations, indicating a high number of pollutants and a very low number of active sites (Yogeshwaran *et al.*, 2021). With further increase in metal ion concentrations, copper metal ion uptake efficiency reached the saturation level, and after that, there were no changes in metal ion removal. Based on the experimental investigations. 20 mg/L concentrated copper metal ion containing solution provides maximum adsorption efficiency using sawdust powder.

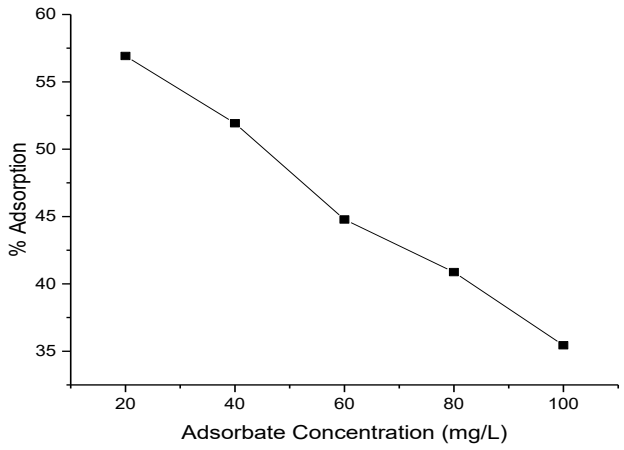

Figure 7. Impact of chromium metal ion uptake by varying Adsorbate Concentration

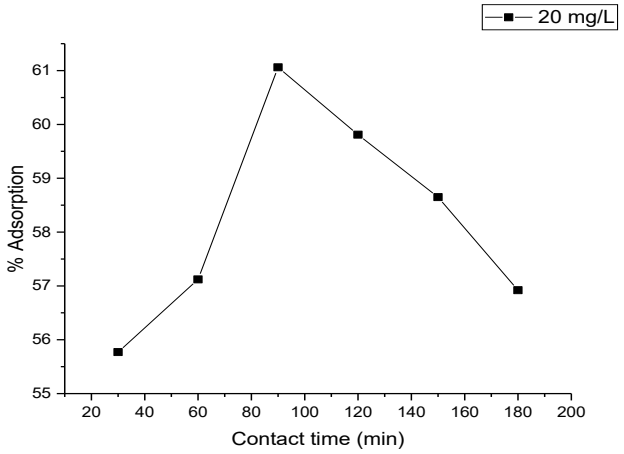

Figure 8. Impact of chromium metal ion uptake by varying contact time

3.8. Impact of adsorption by varying the contact time

The time of contact between copper metal ion solution and activated sawdust adsorbent has been adjusted from 10 to 180 minutes with optimum pH of 2.0, a concentration of 20 mg/L, and an adsorbent dose of 0.6 g/L at 30°C. Figure 8 shows the variations in adsorption efficiency by adjusting the contact time. During the initial time, metal ion uptake was rapid because of highly active site availability in the adsorbent. Later, the active sites were filled with pollutants, and no vacant sites were available on the adsorbent's surface. Due to this, the metal ion uptake was reduced after 90 minutes. A sudden drop in metal ion uptake was noticed, and the adsorption reached saturation (Dulla *et al.*, 2020). There is no metal ion uptake was seen after the saturation point.

3.9. Impact of adsorption by varying the temperature

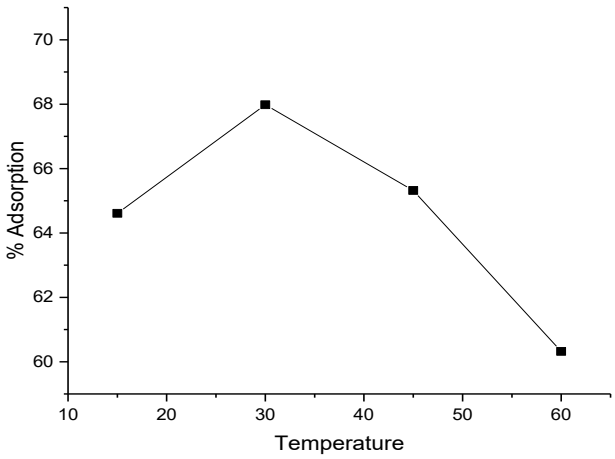

Figure 9. Impact of chromium metal ion uptake by varying temperature

Temperature plays an important role in the efficiency of adsorption. In this study, the copper metal ion solution temperature was adjusted from 15 to 60°C with optimum pH of 2.0, copper ion concentration of 20 mg/L, contact time of 90 minutes and sawdust charcoal dose of 0.6 g/L. Figure 9 shows the efficiency variations of copper metal ion uptake by adjusting the temperature. The maximum efficiency of copper ion adsorption was attained at 30°C; beyond that, the efficiency rate was gradually decreased and attained the equilibrium state. Due to the increase in desorption rate, the decrement in metal ion uptake happened (Hong *et al.*, 2020).

3.10. Impact of adsorption by varying the adsorbent particle size

The particle size variations also affect the efficiency of the adsorption process in batch mode. To check the efficiency variations of copper ion uptake, the size of adsorbent particles was adjusted to 10, 25, 40 & 65 µm levels, and the effect of this study is shown in Figure 5f. The other optimum parameters were taken from previous studies, and the effect was analyzed under various particle sizes. Referring to Figure 10, the maximum adsorption rate was achieved in low particle size (10 µm), and a further increase in particle size reduces adsorption efficiency. Due to the surface area available, the adsorption process and its efficiency will be increased or decreased. The size of adsorbate particles was increased, the surface area was

decreased, and it was very difficult to adsorb the pollutants (Bayuo *et al.*, 2019). Due to this reason, the metal ion uptake was reduced in large particle size.

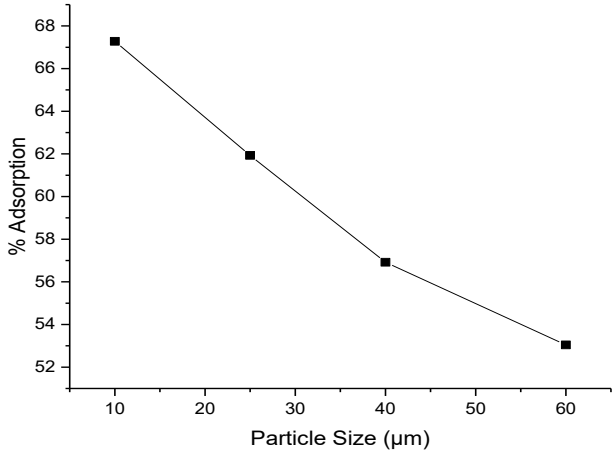

Figure 10. Impact of chromium metal ion uptake by particle size

3.11. Isotherm studies

3.11.1. Langmuir isotherm study

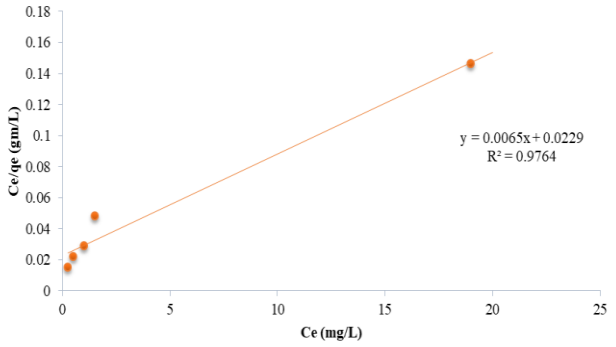

Figure 11. Adsorption isotherm plots of Langmuir Model

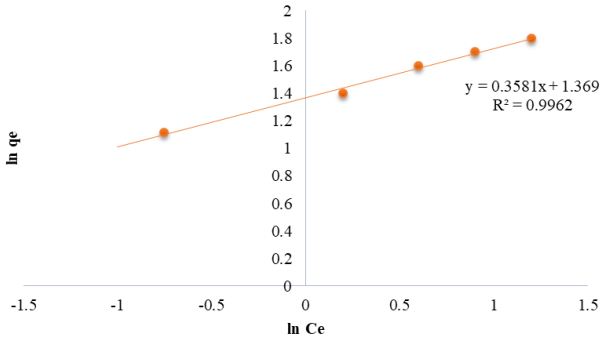

Figure 12. Adsorption isotherm plots of Freundlich Model

The Langmuir isotherm linear plot (C_e/q_e vs C_e) was shown in Figure 11, and the values of capacity & intensity of adsorption (k, q_{max}) were calculated from the slope and deflection of the linear plot. Table 3 shows the various parameters of the Langmuir isotherm model, and the separation parameter obtained in this study is 0.0037, which lies between 0 to 1. The regression value of the linear plot is about 0.9764; is greater than 0.95 may confirm the favorable adsorption process following the monolayer metal ion uptake with heterogeneous nature (Malima *et al.*, 2021).

3.11.2. Freundlich isotherm study

Figure 12 shows the linear plot of the Freundlich isotherm study (ln q_e vs ln C_e), and the energy & capacity of adsorption (n & K_f) values were obtained from slope and deflection values from the linear plot. The adsorption capacity (n) value is 3.284, which lies between 0 and 1, which may authorize the physical adsorption process of copper ions by sawdust powder adsorbent (Wang *et al.*, 2022). The regression value is more than 0.95, and the process of adsorption follows both monolayer and multilayer adsorption process.

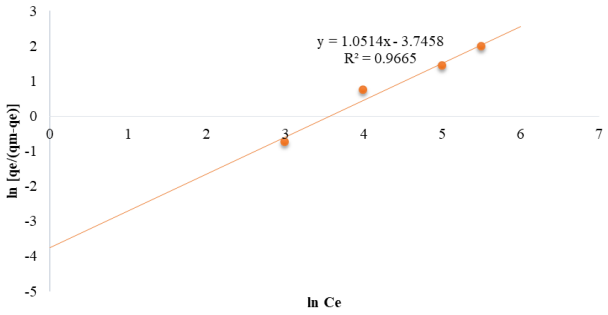

Figure 13. Adsorption isotherm plots of Sips Model

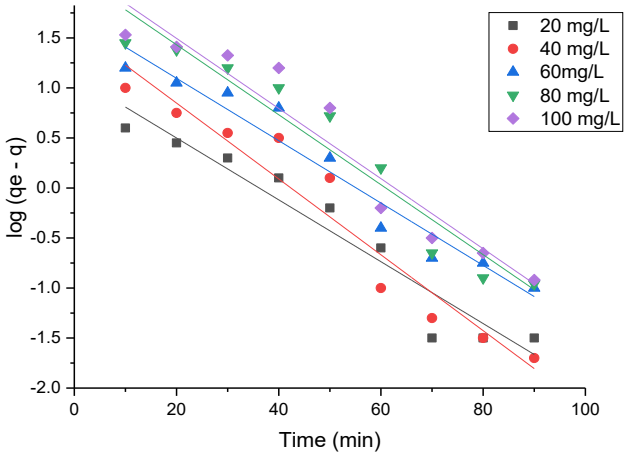

Figure 14. Kinetic plots of Pseudo 1st order model for copper ion uptake using activated sawdust charcoal powder

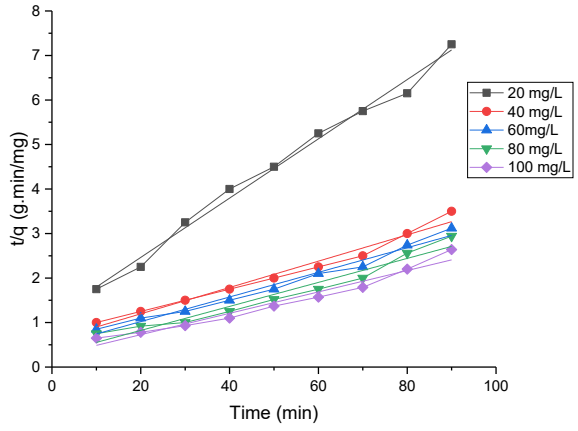

Figure 15. Kinetic plots of Pseudo 2nd order model for copper ion uptake using activated sawdust charcoal powder

3.11.3. Sips isotherm study

Sips model linear plot was shown in Figure 13, and the heterogeneity factor (n) value & regression values obtained from the linear plot are represented in Table 3. The heterogeneity factor decides the process of adsorption follows heterogeneous/homogeneous nature. The R^2 value of the kinetic plot is more than 0.95 may confirm the fitting of this isotherm model. If the n value is less than 1, the adsorption process follows Freundlich fit and n=1; the process follows the Langmuir isotherm fit.

Table 3 Adsorption isotherm constants for copper ion uptake using activated sawdust charcoal powder

S. No.	Model	Parameters	Calculated values
1.	Langmuir	q_{max}	10.353
		K_L	0.434
		R^2	0.9764
2.	Freundlich	K_f	2.895
		n	3.143
		R^2	0.9962
3.	Sips	K_S	16.8235
		β_S	1.4923
		a_S	0.6012
		R^2	0.9665

Table 4 Adsorption kinetic constants of Cu^{2+} uptake using activated sawdust charcoal powder

S. No.	Conc. (mg/L)	Pseudo 1st order			Pseudo 2nd order			
		K (min^{-1})	q_e, cal (mg/g)	R^2	K (g/mg. min) X 10^{-3}	q_e, cal (mg/g)	h (mg/g.min)	R^2
1.	20	0.037	1.96	0.97	18.15	2.18	0.13	0.95
2.	40	0.049	5.49	0.95	15.27	5.39	0.17	0.96
3.	60	0.062	8.49	0.96	10.54	8.48	0.23	0.95
4.	80	0.053	11.38	0.97	5.49	10.24	0.26	0.96
5.	100	0.041	15.25	0.96	2.53	12.53	0.32	0.97

Table 5. Thermodynamic constants of Cu^{2+} metal ion adsorption using sawdust powder

Initial Cu^{2+} Concentration in mg L^{-1}	Enthalpy (ΔH°) KJ mol^{-1}	Entropy (ΔS°) J mol^{-1}	Gibbs Energy (ΔG_o) kJ mol^{-1}			
			15°C	30°C	45°C	60°C
20	78.349	178.392	-15.201	-11.634	-9.853	-7.285
40	40.298	90.536	-11.592	-9.482	-7.034	-6.384
60	19.784	46.024	-9.293	-6.349	-5.895	-4.895
80	13.029	30.265	-6.353	-4.839	-3.473	-3.027
100	9.483	23.593	-4.685	-3.253	-2.845	-2.348

3.12. Kinetic studies

3.12.1. Pseudo first order studies

The kinetic plot of pseudo first order study [(q_e – q) vs t] was shown in Figure 14, and the constants of this kinetic model are represented in Table 4. For this study, the concentration of copper ions in the synthetic solution was adjusted from 20 – 100 mg/L, and the impact on the amount of adsorption was investigated. The regression value of the Lagergren kinetic plot is more than 0.95, which indicates the fitting of this kinetic study with the adsorption process and the constant 'k' was obtained and listed in Table 4. Based on the regression values, the model indicates the process of adsorption reached the saturation point, and there was no further metal ion uptake happened after that (Uduakobong *et al.*, 2020).

3.12.2. Pseudo second order studies

The linear plot of this kinetic model (t/q vs t) was shown in Figure 15, and the constants were calculated and listed in Table 4. The second-order study was similar to first-order studies with a copper ion concentration of 20 – 100 mg/L. The pseudo-second-order study was good in agreement with the copper metal ion adsorption process, and the regression value is more than 0.95, indicating this model's applicability. Based on the applicability of both Pseudo first and second order kinetic models, it was confirmed the adsorption happened in both physical and chemical modes throughout the whole process (Candamano *et al.*, 2022).

3.13. Thermodynamic studies

The thermodynamic plot of copper metal ion adsorption using sawdust powder was shown in Figure 16 with varying metal ion concentrations of 20, 40, 60, 80 & 100 mg/L. The slope and intersection values (ΔH_o and ΔS_o) obtained from the plot are listed in Table 5, along with ΔG_o (Gibbs Energy) values. The enthalpy (ΔH_o) values were found to be positive with negative Gibbs energy (ΔG_o) values, indicating the endothermic reaction of the copper ion adsorption process due to the spontaneous nature of activated sawdust charcoal powder. The entropy (ΔS_o) values found to be positive in Table 5 indicate the solid and liquid uncertainty of metal ion adsorption using activated biochar adsorbent (Phuengphai *et al.*, 2021).

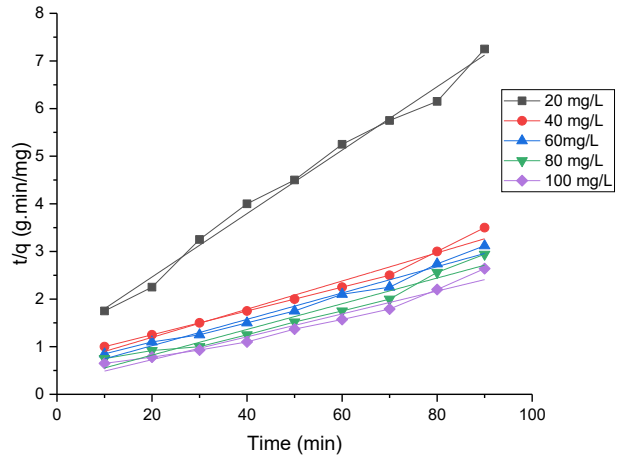

Figure 15. Kinetic plots of Pseudo 2nd order model for copper ion uptake using activated sawdust charcoal powder

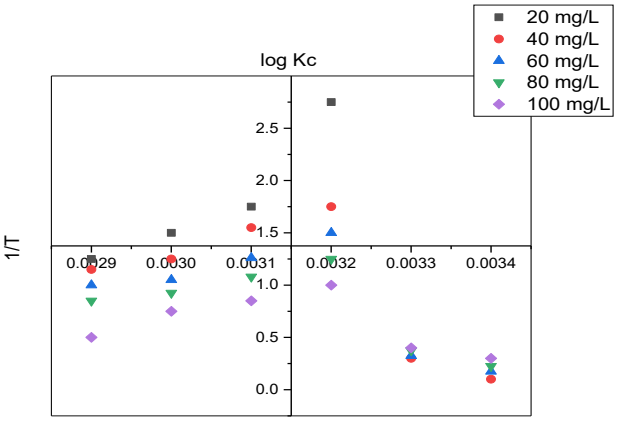

Figure 16. Thermodynamic plot of Cu^{2+} metal ion adsorption using sawdust powder

3.14. Desorption studies

In desorption studies, the copper ions adsorbed by the activated saw dust powder was recovered using concentrated sulfuric acid with various concentrations of 0.1 – 0.4 N. The copper metal ion recovery was very high by increasing the concentration of sulfuric acid up to 0.3N. A decrease in copper recovery was found with increased sulfuric acid concentration. The copper ion recovery attained the saturation point by adding 0.3 N of H_2SO_4, and no further increase in ion regaining was observed after that equilibrium stage (Ngoc Pham *et al.*, 2021). In this experimental study, 0.3 N of H_2SO_4 acid recovered 93.27% of copper ions from the spent adsorbent, and the retrieved copper ions were used for further experimental studies.

4. Conclusion

Biosorption of copper metal ions from the synthetic solution has been investigated using the activated sawdust powder. The activated adsorbent removed 65% of copper metal ions at the optimum pH of 2.0 with a 0.6 g/L adsorbent dose at 90 minutes. Within 90 minutes of contact time, 10 µm size activated adsorbent material removed the maximum amount of copper ions at 30°C. Langmuir, Freundlich and Sips model isotherms were fitted well with the adsorption process, and copper metal ion uptake by the sawdust adsorbent follows both Pseudo first & second order kinetic studies. Based on the isotherm studies, the adsorption process follows monolayer/multilayer adsorption with heterogeneous nature. The positive and negative values of thermodynamic constants suggest the uncertainty of solid and liquid interactions. The amount of copper metal ions was desorbed by adding concentrated sulfuric acid.

References

Ambaye T.G., Vaccari M., van Hullebusch E.D., Amrane A., and Rtimi S. (2021). Mechanisms and adsorption capacities of biochar for the removal of organic and inorganic pollutants from industrial wastewater, *International Journal of Environmental Science and Technology*, **18**, 3273–3294. https://doi.org/10.1007/s13762-020-03060-w.

Batagarawa S.M., and Ajibola A.K. (2019). Comparative evaluation for the adsorption of toxic heavy metals on to millet, corn and rice husks as adsorbents. *Journal of Analytical and Pharmaceutical Research*, **3**, 119–125. Doi: 10.15406/japlr.2019.08.00325.

Bayuo J., Pelig-Ba K.B., and Abukari M.A. (2019) Adsorptive removal of chromium(VI) from aqueous solution unto groundnut shell. *Applied Water Science*, **9**, 107. https://doi.org/10.1007/s13201-019-0987-8.

Benjelloun M., Miyah Y., Evrendilek G.A., and Lairini F.Z.S. (2021). Recent advances in adsorption kinetic models: their application to dye types, *Arabian Journal of Chemistry*, **14**(4), 103031. https://doi.org/10.1016/j.arabjc.2021.103031 .

Candamano S., Policicchio A., Conte G., Abarca R., Algieri C., Chakraborty S., Curcio S., Calabrò V., Crea F., and Agostinobc R.G. (2022). Preparation of foamed and unfoamed geopolymer/NaX zeolite/activated carbon composites for CO2 adsorption, *Journal of Cleaner Production*, **330**, 129843. https://doi.org/10.1016/j.jclepro.2021.129843.

Dey A.K., Dey A., and Goswami R. (2022). Adsorption characteristics of methyl red dye by Na2CO3-treated jute fibre using multi-criteria decision-making approach, *Applied Water Science*, **12**, 179. https://doi.org/10.1007/s13201-022-01700-9.

Dulla J.B., Tamana M.R., Boddu S., Pulipati K., and Srirama K. (2020). Biosorption of copper (II) onto spent biomass of Gelidiella acerosa (brown marine algae): optimization and kinetic studies, *Applied Water Science*, **10** (56). https://doi.org/10.1007/s13201-019-1125-3.

Edet U.A., and Ifelebuegu A.O. (2020). Kinetics, isotherms, and thermodynamic modeling of the adsorption of phosphates from model wastewater using recycled brick waste, *Processes*, **8**, 665. https://doi.org/10.3390/pr8060665.

Eleryan A., Uyiosa Aigbe O., Ukhurebor K.E., Onyancha R.B., Eldeeb T.M., El-Nemr M.A., Hassaan M.A., Ragab S., Osibote O.A., Kusuma H.S., Darmokoesoemo H., and El Nemr A. (2022). Copper(II) ion removal by chemically and physically modified sawdust biochar. *Biomass Conversion and Biorefinery*. https://doi.org/10.1007/s13399-022-02918-y.

Feszterová M., Porubcová L., and Tirpáková A. (2021). The monitoring of selected heavy metals content and bioavailability in the soil-plant system and its impact on sustainability in agribusiness food chains, *Sustainability*, **13**, 7021. https://doi.org/10.3390/su13137021.

Fideles R.A., Teodoro F.S., Xavier A.L.P., Adarme O.F.H., Gil L.F., and Gurgel L.V.A. (2019). Trimellitated sugarcane bagasse: A versatile adsorbent for removal of cationic dyes from aqueous solution. Part II: Batch and continuous adsorption in a bicomponent system, *Journal of Colloid and Interface Science*, **552**(15), 752–763. https://doi.org/10.1016/j.jcis.2019.05.089.

Gunatilake S.K. (2016). Removal of Cr (III) ions from wastewater using sawdust and rice husk biochar pyrolyzed at low temperature. *International Journal for Innovation Education and Research*, **4**(4), 40–54.

Halim A.A., El-Ezaby K.H., El-Gammal M.I., and Saber H.M. (2019). Removal of Fe2+ and Pb2+ ions from wastewater using rice husk-based adsorbents. *Journal of Egypt Academy of Societry and Environmental Development*, **20**, 47–60. Doi: 10.21608/JADES.2019.67694.

Hong J., Xie J., Mirshahghassemi S., and Lead J. (2020). Metal (Cu, Cr, Ni, Pb) removal from environmentally relevant waters using polyvinylpyrrolidone – coated magnetic nanoparticles. *RSC Advances*, **10**, 3266–3276. Doi: https://doi.org/10.1039/C9RA10104G.

Khalid M.W., and Salman S.D. (2019). Adsorption of heavy metals from aqueous solution onto sawdust activated carbon. *Al-Khwarizmi Engineering Journal*, **15**(3), 60–69. https://doi.org/10.22153/kej.2019.04.001.

Khan T.A., Md. Noumana, Dua D., Khan S.A., and Alharthi S.S.(2022). Adsorptive scavenging of cationic dyes from aquatic phase by H3PO4 activated Indian jujube (Ziziphus mauritiana) seeds based activated carbon: Isotherm, kinetics, and thermodynamic study, *Journal of Saudi Chemical Society*, **26**(2), 101417. https://doi.org/10.1016/j.jscs.2021.101417.

Langeroodi N.S., Farhadravesh Z., and Khalaji A.D. (2018) Optimization of adsorption parameters for Fe (III) ions removal from aqueous solutions by transition metal oxide nanocomposite. *Green Chemistry Letters and Reviews*, **11**(4), 404–413. https://doi.org/10.1080/17518253.2018.1526329.

Malima N., Owonubi S.J., Lugwisha E.H., and Mwakaboko A.S. (2021). Thermodynamic, isothermal and kinetic studies of heavy metals adsorption by chemically modified Tanzanian Malangali kaolin clay. *International Journal of Environmental Science and Technology*, **18**(10), 1–16. http://dx.doi.org/10.1007/s13762-020-03078-0.

Pham B.N., Kang J-K., Lee C-G., and Park S-J. (2021). Removal of Heavy Metals (Cd2+, Cu2+, Ni2+, Pb2+) from Aqueous Solution Using Hizikia fusiformis as an Algae-Based Bioadsorbent, *Applied Sciences*, **11**(18), 8604. https://doi.org/10.3390/app11188604.

Pholosi A, Naidoo E.B., and Ofomaja A.E. (2019). Intraparticle diffusion of Cr (VI) through biomass and magnetite coated biomass: A comparative kinetic and diffusion study, *South African Journal of Chemical Engineering*, **32**, 39–55. https://doi.org/10.1016/j.sajce.2020.01.005.

Phuengphai P., Singjanusong T., Kheangkhun N., and Wattanakornsiri A. (2021). Removal of copper (II) from aqueous solution using chemically modified fruit peels as efficient low-cost biosorbents, *Water Science and Engineering*, **14**(4), 286–294. http://dx.doi.org/10.1016/j.wse.2021.08.003.

Pragati, S.S.T., and Pandey L. (2015). Removal of zinc from synthetic wastewater by saw dust as an adsorbent. *International Journal of Innovative Science, Engineering & Technology*, **2**(6), 120–127.

Priya A.K., Yogeshwaran V., Rajendran S., Hoang T.K.A., Soto-Moscoso M., Ghfar A.A., and Bathula C. (2022). Investigation of mechanism of heavy metals (Cr6+, Pb2+& Zn2+) adsorption from aqueous medium using rice husk ash: Kinetic and thermodynamic approach, *Chemosphere*, **286**, 131796. https://doi.org/10.1016/j.chemosphere.2021.131796.

Saruchia and Kumar V. (2019). Adsorption kinetics and isotherms for the removal of rhodamine B dye and Pb+2 ions from aqueous solutions by a hybrid ion-exchanger, *Arabian Journal of Chemistry*, **12**(3), 316–329. https://doi.org/10.1016/j.arabjc.2016.11.009.

Singh J., Dhiman N., and Sharma N.K. (2018). Effect of Fe(II) on the adsorption of Mn(II) from aqueous solution using esterified saw dust: equilibrium and thermodynamic studies. *Indian Chemical Engineer*, **60**(3), 255–268. https://doi.org/10.1080/00194506.2017.1363674.

Sirusbakht S., Vafajoo L., Soltani S., and Habibi S. (2018). Sawdust bio sorption of chromium (VI) ions from aqueous solutions. *Chemical Engineering Transactions*, **70**, 1147–1152. 10.3303/CET1870192.

Velusamy S., Roy A., Sundaram S., and Mallick T.K. (2021). A Review on Heavy Metal Ions andContaining Dyes Removal ThroughGraphene Oxide-Based AdsorptionStrategies for Textile WastewaterTreatment. The chemical record, 21: 1 – 42. Doi: https://doi.org/10.1002/tcr.202000153

Venkatraman Y., and Priya A.K. (2021). Removal of heavy metal ion concentrations from the wastewater using tobacco leaves coated with iron oxide nanoparticles, *International Journal of Environmental Science and Technology*, **19**, 2721–2736. https://doi.org/10.1007/s13762-021-03202-8.

Wang C., Wang X., Li N., Tao J., Yan B., Cui X., and Chen G. (2022). Adsorption of Lead from Aqueous Solution by Biochar: A Review. *Clean Technologies*, **4**, 629–652. https://doi.org/10.3390/cleantechnol4030039.

Yahya M.D., Aliyu A.S., Obayomi K.S., Olugbenga A.G., and Abdullahi U.B. (2020) Column adsorption study for the removal of chromium and manganese from electroplating wastewater using cashew nutshell adsorbent. *Chemical Engineering*, **7**: 1748470. Doi: https://doi.org/10.1080/23311916.2020.1748470.

Yaseen D.A., and Scholz M. (2018). Textile dye wastewater characteristics and constituents of synthetic effluents: a critical review, *International Journal of Environmental Science and Technology*, **16**, 1193–1226. https://doi.org/10.1007/s13762-018-2130-z.

Yogeshwaran V., and Priya A.K. (2021). Experimental studies on the removal of heavy metal ion concentration using sugarcane bagasse in batch adsorption process, *Desalination and Water Treatment*, **224**, 256–272. 10.5004/dwt.2021.27160.